Available online at www.sciencedirect.com
SCIENCE DIRECT®
ELSEVIER
European Journal of Mechanics B/Fluids 22 (2003) 259–270

Optimal linear growth in the asymptotic suction boundary layer

Jens H.M. Fransson *,[1], Peter Corbett

IMFT, allée du Pr. Camille Soula, 31400 Toulouse, France

Received 26 September 2002; accepted 18 March 2003

Abstract

A variational technique in the temporal framework is used to study initial configurations of disturbance velocity which maximize perturbation kinetic energy in the asymptotic suction boundary layer (ASBL). These optimal perturbations (OP) excite significant and remarkably persistent transient growth, on the order of that which occurs in the Blasius boundary layer (BBL). In contrast, classical modal analysis of the ASBL predicts a critical Reynolds number two orders of magnitude larger than that for the BBL. As in other two-dimensional boundary layer flows, disturbances undergoing maximum amplification are infinitely elongated in the direction of the flow and take the form of streamwise-oriented vortices which induce strong variations in the streamwise perturbation velocity (streaks). The Reynolds number dependence of the maximum growth, and the best choice of scaling for the spanwise wavenumber of the perturbation causing it, are elucidated. There is good agreement between the streak resulting from OP and disturbances measured in experiments in which the asymptotic suction boundary layer is subject to free stream turbulence (FST). This agreement is shown to improve as the level of FST increases.

Keywords: Transient growth; Boundary layer; Asymptotic suction; Optimal perturbations; Streaks

1. Introduction

A boundary layer subject to a wall-normal flow is encountered in many applications, e.g., filtration through porous membranes, and laminar flow control via suction through discrete holes or a permeable surface. Potential reductions in viscous drag on the order of 60% to 80% provided a strong motivation for early workers to concentrate on the latter case, for which Meridith and Griffith[2] found a general solution in the asymptotic limit of constant suction. Later Iglisch[2] extended this work to the non-similar flow arising before the asymptotic state establishes itself, and outlined a method for finding the velocity profile corresponding to an arbitrary suction distribution.

The application of optimal control theory to laminar flow control has sparked a renaissance in the field (Bewley [2]). An extensive amount of work has been done on the subject of flow control in general and the interested reader is addressed to Moin and Bewley [3], Joslin et al. [4], Joslin [5], Lumley and Blossey [6], Balakumar and Hall [7], Högberg [8], and Lundell [9], just to mention a few works on both experimental and numerical control. Pralits et al. [10] and Walther et al. [11] have recently outlined methods in which modifications to the boundary layer flow by spatially-varying steady suction create conditions which stabilize linear disturbances. This approach contrasts with earlier work in which the disturbances themselves are the target of some rationally directed control activity (Abergel and Témam [12], Bewley and Liu [13]).

The difficulties of sensing boundary layer disturbances in an aerospace setting on the one hand, and the inherent complexity of a system capable of delivering variable suction at an arbitrary position on a lifting surface on the other, pose formidable

* Corresponding author.
E-mail address: jens.fransson@mech.kth.se (J.H.M. Fransson).
[1] Permanent address: KTH Mechanics, 10044 Stockholm, Sweden.
[2] These references are taken from Schlichting [1].

0997-7546/03/$ – see front matter
doi:10.1016/S0997-7546(03)00033-5

implementation challenges with technology available today. The simple case where the boundary layer is subject to uniform, constant suction, as initially envisioned by the pioneers in the field, is far more likely to find application in practice. It is also the focus of recent experimental and theoretical work by Fransson and Alfredsson [14], who investigated the linear stability characteristics of the flow using classical spatial stability theory (Drazin and Reid [15], Schmid and Henningson [16]). They determined the behaviour of Tollmien–Schlichting waves, and observed disturbances evoked by varying levels of free stream turbulence (FST, whose intensity is typically quantified by the parameter $Tu = u_{\rm rms}/U_\infty$).

Additional terms in the familiar Orr–Sommerfeld/Squire system describing linear stability appear as a consequence of the normal velocity component, however it has long been known that the change in shape of the mean streamwise velocity profile is the main reason for the altered stability characteristics of the flow (Drazin and Reid [15]). That this change is considerable is reflected by a two order of magnitude increase in critical Reynolds number (Hocking [17]). In turn, this indicates that modal Tollmien–Schlichting disturbances are significant in flows where the free stream velocity dominates the suction velocity.

At moderate flow régimes likely to arise in applications, attention must then turn to other linear growth mechanisms. Since Fransson and Alfredsson [14] report the presence of streaks in asymptotic suction boundary layers subject to FST, it is natural to inquire whether and to what degree this flow is capable of sustaining algebraic or transient growth, of which streaks are a characteristic signature (see Westin [18], Matsubara and Alfredsson [19], and their references for a complete review of the phenomenon in the Blasius boundary layer (BBL)).

Algebraic growth is a consequence of the non-normality of the governing differential operator: as the normal modes are not orthogonal, constructive and destructive interference may give rise to transients before the asymptotic state described by modal theory sets in (Schmid and Henningson [16]). Butler and Farrell [20] pioneered the study of optimal perturbations (OP) in shear flows; their findings and those of later workers indicate that the initial conditions which maximize perturbation kinetic energy are streamwise-oriented vortices which produce streaks (variations in the streamwise perturbation velocity). Ever since the transient growth and its linear physical mechanism was described by Ellingsen and Palm [21], and Landahl [22] a number of works has been done on the topic. Among the earlier ones are, e.g., Hultgren and Gustavsson [23], Gustavsson [24], Reddy and Henningson [25], and Trefethen et al. [26]. For more recent publications on the subject see, e.g., Luchini [27], Reshotko [28], and Andersson et al. [29].

In the following, OP are sought for the asymptotic suction boundary layer (ASBL) using a direct-adjoint technique in the temporal framework. This method has been employed previously to investigate the Falkner–Skan–Cooke family of boundary layers (Corbett and Bottaro [30,31]). For the ASBL the parallel flow approach is exact and no local approximations are made. The results are then compared with experimental measurements made by Fransson [32], and good agreement between the computed and measured disturbances in the boundary layer is observed.

2. Asymptotic suction boundary layer

This work focuses on events in the steady flow of an incompressible fluid over a permeable flat plate through which a normal velocity is applied, and in particular to the region where the boundary layer ceases to evolve in the streamwise direction. The general situation is depicted in Fig. 1. In this two-dimensional flow continuity is satisfied directly, provided the streamwise

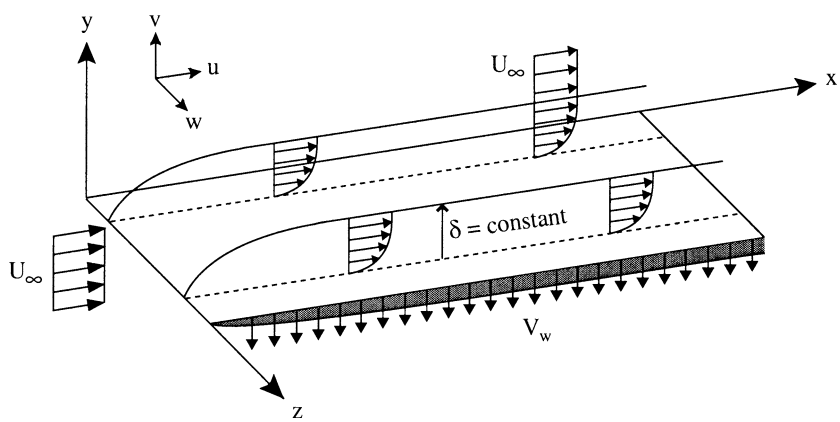

Fig. 1. Schematic of the flow field over a flat plate subjected to constant suction. The coordinate system used in this work is shown, along with the corresponding velocity components.

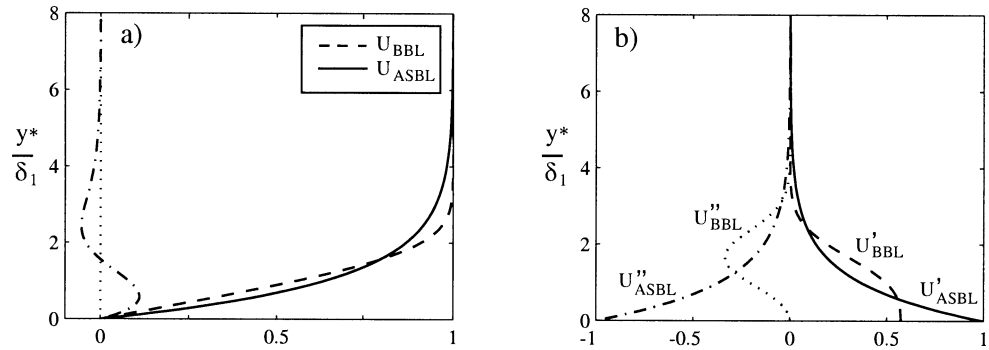

Fig. 2. (a) Velocity profiles for the asymptotic suction (ASBL) and Blasius (BBL) boundary layers, with their difference indicated by the dash-dotted line. (b) First and second derivatives. Superscript $*$ indicates dimensional quantities.

velocity varies only in y and the wall-normal velocity is constant. The subsequent simplification of the x-momentum equation permits its direct integration,

$$U(y) = U_\infty\left[1 - \exp\left(\frac{yV_\mathrm{w}}{\nu}\right)\right], \tag{1}$$

where U_∞ is the free stream velocity, V_w is the normal velocity applied at the wall, and ν is the kinematic viscosity. Physical solutions are associated only with the suction case $V_\mathrm{w} < 0$ (see Schlichting [1], White [33], and their references for more details). The displacement and momentum thicknesses,

$$\delta_1 = -\frac{\nu}{V_\mathrm{w}} \quad \text{and} \quad \delta_2 = \frac{\delta_1}{2},$$

are constant, as is the boundary layer thickness. In this flow the wall-directed convection exactly balances the growth of the shear layer through viscous diffusion. The resulting streamwise velocity profile is fuller than the Blasius boundary layer, as shown in Fig. 2.

The Reynolds number based on δ_1 becomes

$$R = \frac{U_\infty\delta_1}{\nu} = -\frac{U_\infty}{V_\mathrm{w}}, \tag{2}$$

and is used throughout this investigation.

3. Optimization problem

Of interest is the transient behaviour of unsteady three-dimensional velocity perturbations $\tilde{\mathbf{u}}(x, y, z, t) = [\tilde{u}, \tilde{v}, \tilde{w}]$ in a steady incompressible parallel base flow $\mathbf{U}(y) = [U, V_\mathrm{w}, 0]$, which are described by the Navier–Stokes equations linearized about the base state. The ASBL is parallel, but to treat the spatially developing BBL as parallel is an approximation which is only valid as long as the disturbance varies on a length scale which is much smaller than that of the base flow.

Since the base flow $\mathbf{U}$ has two components, terms involving V_w arise and the classical Orr–Sommerfeld/Squire equations are no longer valid. These extra terms can easily be taken into consideration provided the unknowns are scaled with respect to U_∞ and δ_1, as V_w can then be replaced by $-1/R$ (cf. (2)). Furthermore, the system of linearized Navier–Stokes equations describing $\tilde{\mathbf{u}}$ can be simplified considerably by eliminating the perturbation pressure and introducing the wall-normal perturbation vorticity, $\tilde{\eta} = \partial\tilde{u}/\partial z - \partial\tilde{w}/\partial x$.

The resulting system for $\tilde{\mathbf{v}} = [\tilde{v}, \tilde{\eta}]$ can, upon assuming periodicity in the stream- and spanwise directions,

$$\tilde{\mathbf{v}}(x, y, z, t) = \mathbf{v}(y, t)\exp(\mathrm{i}\alpha x + \mathrm{i}\beta z),$$

(with $\alpha, \beta \in \mathbb{R}$ the corresponding stream- and spanwise wavenumbers), be written

$$\left[\left(\frac{\partial}{\partial t} + \mathrm{i}\alpha U - \frac{1}{R}\frac{\partial}{\partial y}\right)\Delta - \mathrm{i}\alpha\frac{\mathrm{d}^2U}{\mathrm{d}y^2} - \frac{1}{R}\Delta^2\right]v = 0, \tag{3}$$

$$\left[\frac{\partial}{\partial t} + \mathrm{i}\alpha U - \frac{1}{R}\frac{\partial}{\partial y} - \frac{1}{R}\Delta\right]\eta = -\mathrm{i}\beta\frac{\mathrm{d}U}{\mathrm{d}y}v. \tag{4}$$

Here $\Delta = \partial^2/\partial y^2 - k^2$ represents the Laplacian operator, where $k^2 = \alpha^2 + \beta^2$, and the grouping $-(1/R)\partial/\partial y$ represents wall-normal convective effects. Perturbations are assumed to be zero at the wall and to vanish far from the wall. As a consequence homogeneous Dirichlet boundary conditions apply to $\mathbf{v}$, and from continuity it is seen that additional homogeneous Neumann conditions apply to v.

Initial conditions $\mathbf{v}_0 = \mathbf{v}_0(y)$ for (3) are sought which undergo maximum relative amplification over a given time span, $t \in [0, \tau]$. The metric used here is the growth,

$$G(\tau) = \frac{E(\tau)}{E(0)}, \tag{5}$$

or ratio of final to initial perturbation kinetic energy densities,

$$E(t) = \frac{1}{2}\int_0^\infty (\bar{u}\cdot u + \bar{v}\cdot v + \bar{w}\cdot w)\,\mathrm{d}y = \frac{1}{2k^2}\int_0^\infty (-\bar{v}\Delta v + \bar{\eta}\cdot\eta)\,\mathrm{d}y.$$

Above, overbars indicate conjugate transpose quantities.

The procedure for determining $\mathbf{v}(y,0) = \mathbf{v}_0$ which maximizes the ratio (5) while satisfying (3) and its boundary conditions is described in detail in Corbett and Bottaro [31], to which the interested reader is referred (alternative methods in the temporal and spatial frameworks are reported in Butler and Farrell [20] and Andersson et al. [34], respectively). Here it is simply noted that the constraints on the extremization of G are enforced by introducing Lagrange multipliers, or adjoint variables, for each of the constraints. An iterative procedure is then used to maximize G. One starts from an arbitrary guess for $\mathbf{v}_0$ and integrates (3) from $t = 0$ to $t = \tau$. At this point transfer relations,

$$a(y,\tau) = -\frac{1}{2k^2E(0)}v(y,\tau), \qquad b(y,\tau) = \frac{1}{2k^2E(0)}\eta(y,\tau),$$

from $\mathbf{v}$ to its adjoint $\mathbf{a}(y,t) = (a,b)^{\mathrm{T}}$ are applied. The adjoint field's behaviour is described by,

$$\left[\left(\frac{\partial}{\partial t} + \mathrm{i}\alpha U - \frac{1}{R}\frac{\partial}{\partial y} + \frac{1}{R}\Delta\right)\Delta + 2\mathrm{i}\alpha\frac{\mathrm{d}U}{\mathrm{d}y}\right]a = -\mathrm{i}\beta\frac{\mathrm{d}U}{\mathrm{d}y}b, \tag{6}$$

$$\left[\frac{\partial}{\partial t} + \mathrm{i}\alpha U - \frac{1}{R}\frac{\partial}{\partial y} + \frac{1}{R}\Delta\right]b = 0, \tag{7}$$

where the boundary conditions on $\mathbf{a}$ are analogous to those on $\mathbf{v}$. Integrating the adjoint system (6) from $t = \tau$ to $t = 0$, another set of transfer relations

$$v_0(y) = -\frac{2k^2E(0)^2}{E(\tau)}a(y,0), \qquad \eta_0(y) = \frac{2k^2E(0)^2}{E(\tau)}b(y,0),$$

provides an estimate for $\mathbf{v}_0$. The procedure is repeated until $\mathbf{v}_0$ converges, which requires few iterations in general.

4. Results

Before presenting results, some nomenclature is introduced for clarity in the discussion to follow. In a mean flow parameterized by R, what distinguishes an OP for the period $t = \tau$ from all other valid initial conditions described by the wavenumber pair (α, β) is that it maximizes the growth at the end of the interval, $G(\tau)$. The procedure outlined in Section 3 produces a global maximum of G as argued by Luchini [27].

Below, the words 'local' and 'global' are applied in a different context to describe OP: in the following these words will refer to periods of time. The OP for an arbitrary interval is referred to as a *local* optimal,

$$\sigma(\tau) \equiv \max_{\forall v_0(\alpha,\beta)} G(\tau),$$

whereas the largest growth achievable for perturbations described by a given wavenumber pair in the same mean flow is termed a *global* optimal,

$$\gamma = \sigma(t_\gamma) \equiv \max_{\forall t}\sigma(t),$$

where t_γ is time at which this growth occurs. The largest transient growth possible at R is experienced by the *maximum* optimal,

$$\Gamma = \gamma(t_\Gamma) \equiv \max_{\forall\alpha,\beta}\gamma(t_\gamma),$$

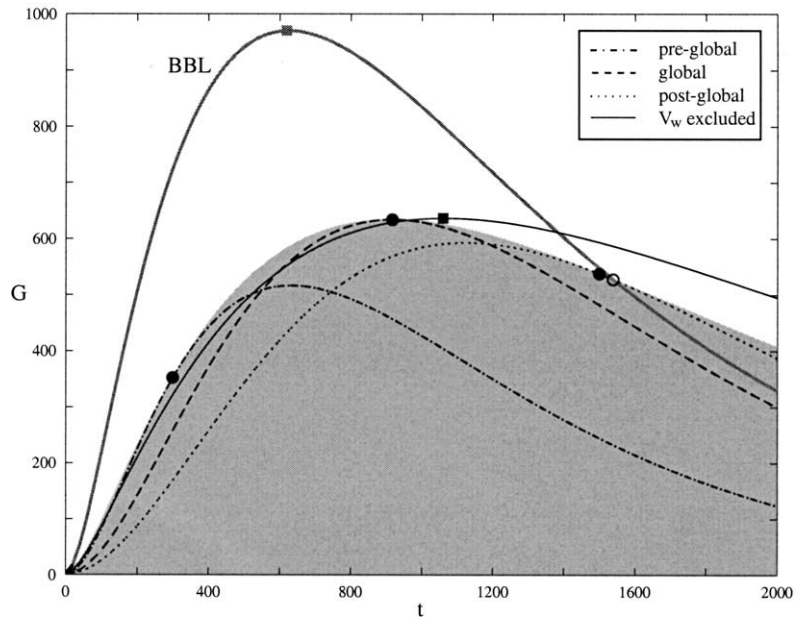

Fig. 3. Local and global OP growth in the ASBL ((α, β) = (0,0.53) at $R = 800$, the shaded region represents the envelope of local optimum growth. The grey line is the envelope of local optimum growth in the BBL ((α, β) = (0,0.65)) at $R = 800$. The individual cases are discussed further in the text.

and is a characteristic quantity of the base flow. Its parameters are denoted t_Γ, α_Γ and β_Γ. Finally, the 'response' of an optimal perturbation is the state of the disturbance at the time for which it is optimal (i.e., τ or t_γ or t_Γ).

The distinctions drawn above are illustrated in Fig. 3. The shaded region represents the envelope of growth attained by local optimals with $\alpha = 0$, $\beta = 0.53$ in the ASBL at $R = 800$. The three curves entirely within this region show the temporal evolution of two local optimals and the global optimal, these are denoted pre-global, post-global and global, respectively. Symbols indicate the times for which they are optimal, demonstrating that locally optimal growth seldom coincides with the maximum growth experienced by the perturbation.

The global optimal shown in Fig. 3 corresponds to the maximum optimal for the ASBL at $R = 800$, no other perturbation experiences more algebraic amplification. The solid grey curve is the analogue of the shaded region for the BBL ($\alpha = 0$, $\beta = 0.65$ at $R = 800$). Evidently, the ASBL is capable of sustaining significant transient growth on the order of that experienced in the BBL. This is in sharp contrast to the situation for modal disturbances: Hocking [17] shows that the critical Reynolds number in the ASBL is two orders of magnitude larger than in the BBL. The strong damping effect of suction on Tollmien–Schlichting waves evidently does not carry over to algebraically excited disturbances.

The difference in transient growth characteristics between the ASBL and the BBL can be attributed to the change in shape of the mean streamwise velocity profile. The solid black line partially within the shaded area in Fig. 3 traces the temporal evolution of the global maximum optimal perturbation ($\Gamma = 636$ at $t_\Gamma = 1065$, with $\alpha = 0$, $\beta = 0.50$) in a hypothetical flow with no suction but an identical U-velocity profile to the ASBL. Effectively, this exercise demonstrates that the additional terms due to V_w in (3) and (6), required to obtain the correct physics, only bring about a small change in the overall result.

Transient growth is not restricted to disturbances infinitely elongated in the streamwise direction. Fig. 4 shows that perturbations exhibiting periodicity in the streamwise direction also experience substantial algebraic excitation. The rapid decrease in t_γ away from the β axis shows that such perturbations reach their maximum amplitude earlier than those undergoing the most amplification, as a consequence they may play a significant role in flows subject to forcing which excites them preferentially.

The physical mechanism behind algebraic growth in the ASBL is identical to that found in previous work on transient growth (Butler and Farrell [20], Andersson et al. [34]). This is seen from the optimal perturbation velocity profiles shown in Fig. 5 and their respective responses at t_γ for the local and global optima of Fig. 3 (cf. Table 1 for a full parameterization of these disturbances). It is possible to discern that the OP take the form of streamwise-oriented vortices, with perturbation velocities distributed primarily in the crossflow plane. In contrast, the response is consistent with a streak, producing a large variation in streamwise perturbation velocity. A physical explanation for this was advanced by Landahl [22], who noted that such initial configurations of perturbation velocity are ideally suited to 'lift-up' low-speed fluid into relatively faster flow and

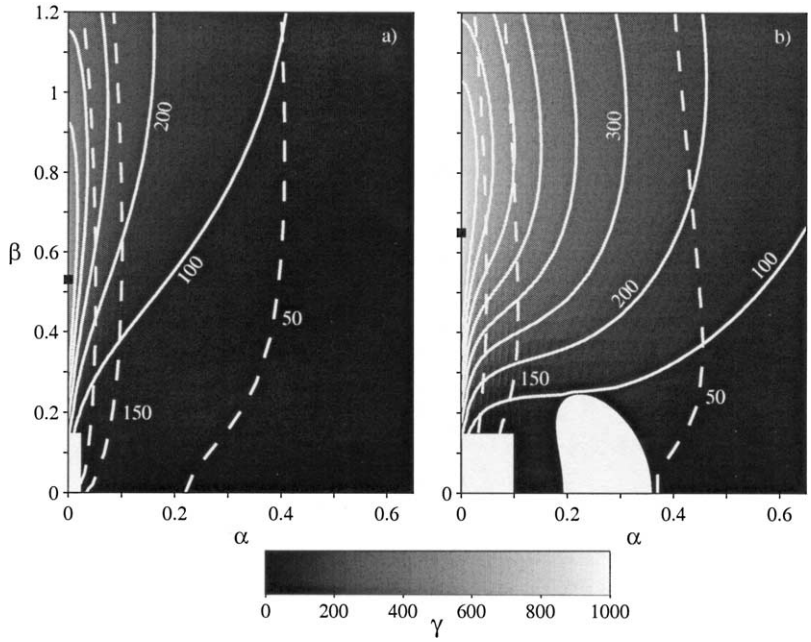

Fig. 4. Contours of global optimal growth in the wavenumber plane at $R = 800$ for (a) the ASBL, (b) the BBL. The empty rectangles near the origin are uncalculated areas, and the empty region about $\alpha \approx 0.3$ in the latter case indicates the presence of exponentially amplified disturbances. Level lines of γ are solid, those of t_γ dashed. The increment between all level lines is 100.

Table 1
Parameterization of the OP at $R = 800$ whose growth is shown in Fig. 3. 'Max' denotes a global maximum, the other fields denote local maxima. In all of these cases $\alpha \equiv 0$

Flow		β	γ	t_γ
BBL	max	0.65	969.9	625.7
ASBL	pre-max	0.53	352.1	300.0
	max	0.53	633.9	917.7
	post-max	0.53	537.7	1500.0

vice versa, exchanging momentum and generating a streak, an effect illustrated in Fig. 6 for the maximum optimal in the ASBL at $R = 800$. Also shown in Fig. 5 are the perturbation velocity profiles for the BBL (given by solid lines). It is interesting to compare the global OP in the ASBL and the BBL, i.e., the dashed and solid lines. Whereas the OP profile maxima for all ASBL cases are located higher above the plate than their BBL counterparts, the reverse holds for the u-component of the response. The time evolution of all perturbation components of the maximum optimal in the ASBL case is illustrated in Fig. 7. The strong initial v- and w-components decay quickly, while the u-component grows until reaching its maximum at $t_\gamma \approx 920$ (coinciding with the maximum energy), decaying slowly thereafter. The pressure perturbation, always largest at the surface, peaks rapidly and decays downstream.

With the scaling employed by Gustavsson [24] to analyse the growth of the vorticity one can show that t_Γ will scale linearly and Γ quadratically with R (Schmid and Henningson [16]). These trends are confirmed for the BBL and ASBL in Fig. 8, where results for several different R have been reduced using both integral length scales. While either scaling is adequate to collapse the data for a given type of boundary layer flow, it is interesting that the spanwise wavenumber associated with maximum growth is nearly independent when scaled with momentum thickness. Similar behaviour has been observed in the Falkner–Skan boundary layer (Corbett and Bottaro [30]). Considering the fact that in the ASBL flow the equations are exact (i.e., no local approximation is invoked) the collapse of the curves in Fig. 8 indicates that boundary layer scales would be appropriate to model the physics of this problem even for R as small as 200. By transferring this argument to the BBL, this result provides a firm ground for the asymptotic (boundary-layer-based) analysis by Andersson et al. [34] and Luchini [27]. Fitting the results for maximum global growth at various R, one obtains the coefficients reported in Table 2. The minor discrepancy in the results reported for the Blasius case may be due to differences in optimization method, numerical discretization, or problem formulation.

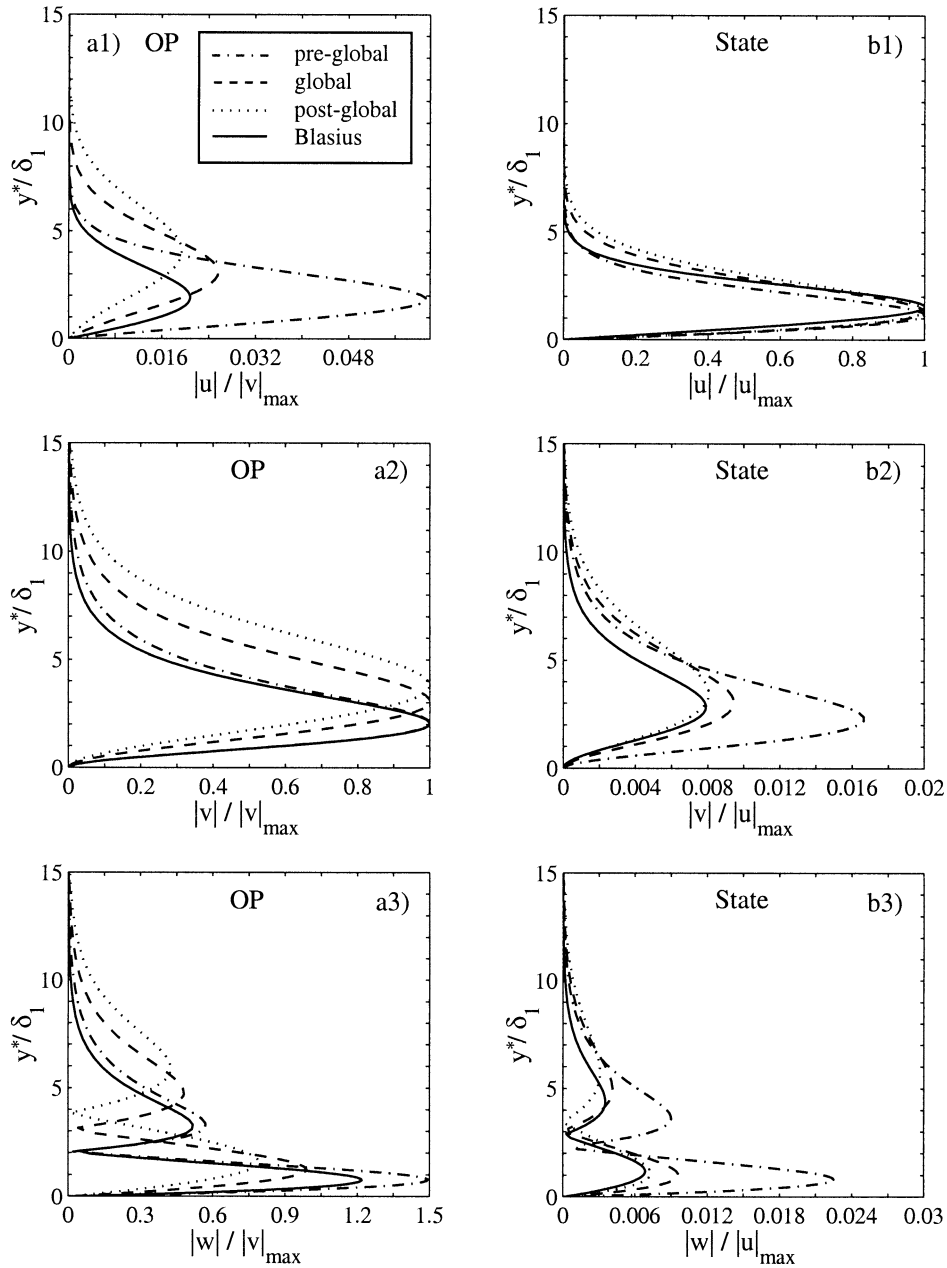

Fig. 5. (a) Perturbation velocity profiles for the pre-global, global and post-global OP in the ASBL and the global OP in the BBL at $R = 800$, (b) their respective states at their respective t_γ (cf. Table 1), marked with symbols in Fig. 3). The line-types of the pre-global, global and post-global profiles correspond to their amplification curves in Fig. 3.

From Table 2 it is evident that in comparison to the case with no suction, the ASBL supports less algebraic growth and that this takes longer to develop. However, it is noticeable in Fig. 3 that as t becomes large more growth is experienced by the transient disturbances in the ASBL than in the BBL. The point of intersection between ASBL and BBL growth curves (cf. the ∘-symbol in Fig. 3) scales as t_Γ and Γ mentioned previously. As this behaviour occurs for all R, it also occurs for all times, including the shorter intervals for which the parallel flow approximation in the BBL is a good one. The coefficients for the intersection relation with respect to t_Γ and Γ are given in Table 2.

The ASBL is one case in which the algebraic growth mechanism presents the only viable linear route to transition at Reynolds numbers of practical interest. In this context it is reasonable to compare the optimal response state to disturbances measured

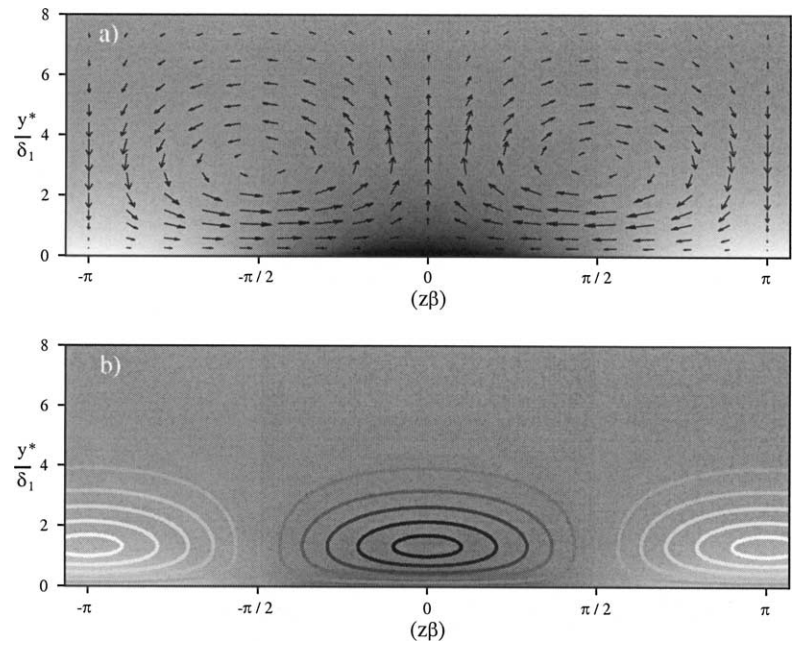

Fig. 6. Evolution of the global OP for the ASBL at $R = 800$ in the crossflow plane, illustrating the lift-up mechanism. (a) The crossflow components of the OP superposed on the perturbation pressure field (dark shading corresponds to low pressure). (b) u-contours of the response (dark lines correspond to low velocity) similarly overlaid on p, at t_γ.

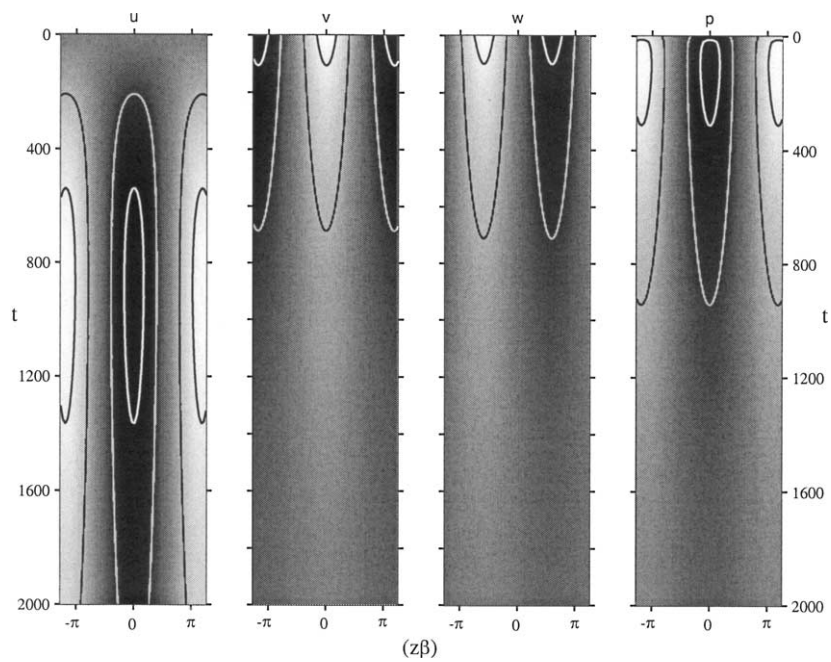

Fig. 7. The time evolution of each perturbation component plotted in the zt-plane at the y-position above the wall where its maximum is found (normalized such that the maximum over all time is unity). Light shading indicates areas of positive perturbation quantities, and contour lines at ± 0.9 and ± 0.5 are shown. $|(u, v, w, p)|_{\max} = (10.8226, 0.25773, 0.25471, 7.4409 \times 10^{-7})$.

inside the boundary layer (cf. §6 of Luchini [27] for more details). Experiments on the ASBL subject to three different levels of FST were conducted by Fransson [32]. Three different turbulence generating grids situated upstream of the leading edge of the flat plate were used to generate the different FST intensities (Tu). The first 0.36 m of the plate is impermeable, after which

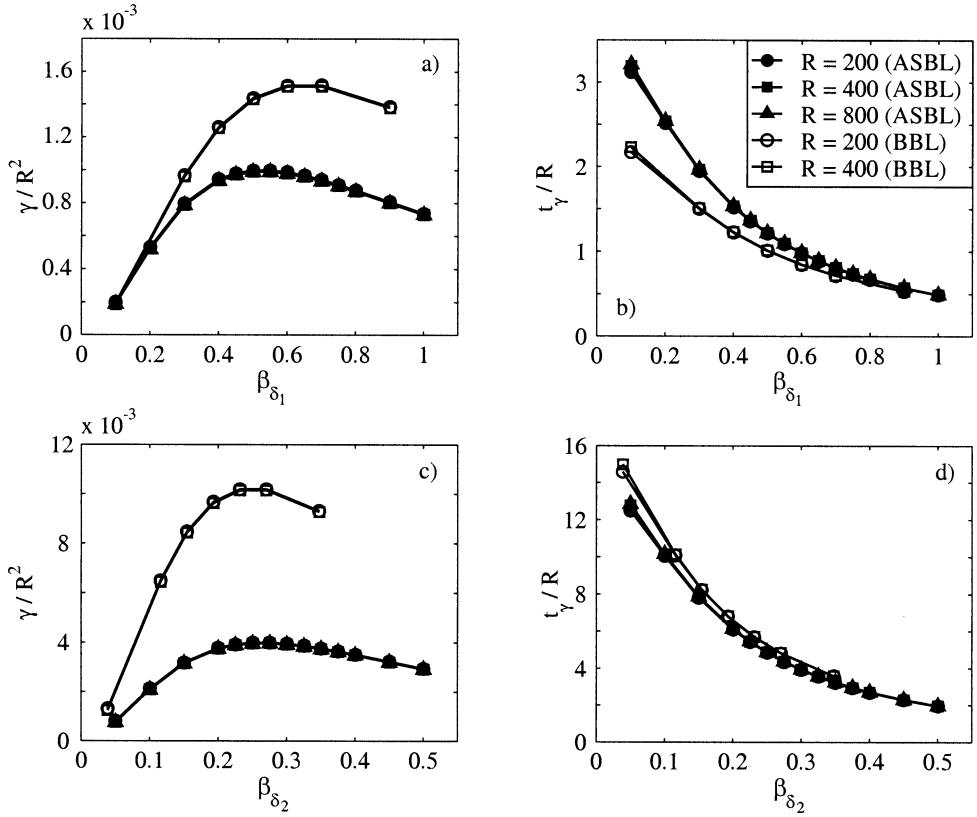

Fig. 8. Behaviour of γ and t_γ with variations in the spanwise wavenumber. (a) and (b) scaled using δ_1, the displacement thickness. (c) and (d) using δ_2, the momentum thickness.

Table 2
Reynolds number dependence of the maximum global optimal energy growth (Γ) and the time (t_Γ) at which this appears for the Blasius-, asymptotic suction boundary layer, and their intersection (see text)

Flow	$\Gamma \times 10^3$	t_Γ	β
BBL, Butler and Farrell [20]	$1.50R^2$	$0.778R$	0.65
BBL	$1.51R^2$	$0.781R$	0.65
ASBL	$0.99R^2$	$1.147R$	0.53
BBL, ASBL intersection	$0.82R^2$	$1.920R$	0.53

uniform suction through a porous plastic plate material causes an asymptotic boundary layer to develop. The suction is such that $R = 347$ when $U_\infty = 5\text{m/s}$, and measurements are carried out using hot-wire anemometry.

The experimentally observed streaks are not stationary in space nor in time. Thus, from two-point spatial correlation measurements a spanwise correlation function may be extracted and the position between the two probes where a distinct minimum in the correlation function is observed (which is quite clear in laminar boundary layers) may be interpreted as half the dominating spanwise wavelength of the streaks (i.e., $= \pi/\beta$). Experimentally, a small increase of the spanwise scale with the downstream distance is observed and the scale seems to vary inversely with the level of free stream turbulence (cf. Fransson and Alfredsson [14]). Fig. 9 compares perturbation velocity profiles of two different OP with measurements at three different streamwise stations when $Tu = 1.4\%$. The agreement is good between the theoretical predictions, corresponding to the maximum global optimal for this flow and the global optimal at the measured streak spacing, and measurements carried out at three x-stations. As might be expected the concordance is slightly better for the optimal whose spanwise periodicity matches the experimental conditions.

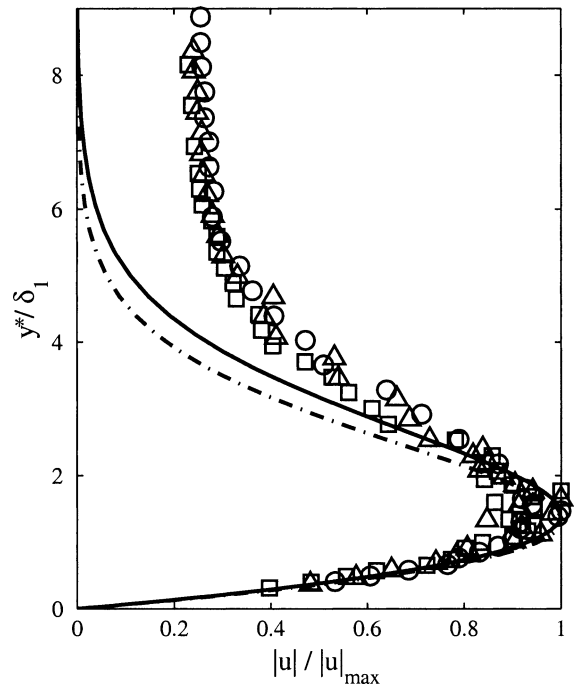

Fig. 9. Streamwise perturbation velocity profiles at $R = 347$. Lines are OP response (i.e., disturbance at t_γ: solid line for $\beta = 0.33$, the measured streak separation; dash-dotted for $\beta = 0.53$, the maximum global optimal), symbols represent experimental data (u_{rms}) at different downstream positions, $x = 1$m (○), 1.6m (△), 2m (□) for a flow with $Tu = 1.4\%$. Experimental data from Fransson [32].

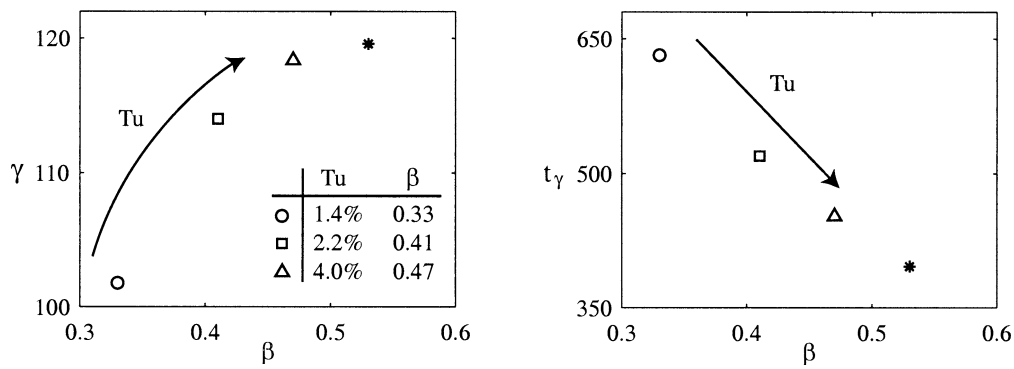

Fig. 10. Computed γ and corresponding t_γ for four different β at $R = 347$. The open symbols indicate spanwise wavenumbers obtained from experiments at different Tu, whereas the global maximum at this R is shown by $*$.

In comparing theory to measurement, differences in free-stream disturbance amplitude between the BBL and ASBL are apparent (cf. Andersson et al. [34], Luchini [27], Matsubara and Alfredsson [19]). The explanation is simple: in the BBL, perturbations within the boundary layer grow with x, and since the data is normalized to unity the free-stream disturbance amplitude decreases. In contrast, disturbance growth within the ASBL ceases as the asymptotic régime is approached for that particular suction velocity, and so a similar scaling causes the disturbance profiles to collapse in the free stream (see Fransson and Alfredsson [14]).

As mentioned above, the magnitude of Tu appears to have a significant effect on the measured streak spacing. Fig. 10 shows that the theoretically predicted spanwise wavenumber for the maximum global OP is approached as Tu increases. In this figure the different β are extracted from the experiments (corresponding to a particular Tu) and used as an input to the OP-calculation. It is noteworthy that the maximum achievable growth varies little with large changes in β, on the other hand t_γ decreases dramatically.

It should be pointed out that the receptivity process giving rise to streaky structures is very complex and far from fully understood. There are many parameters influencing the process that are hard to control in an experiment when changing *Tu*. Amongst them are the integral and Taylor length scales of the FST that are impossible to keep constant, even when an active grid (with a variable upstream injection of secondary fluid in order to change *Tu*) with fixed mesh width and bar geometry is used (cf. Fransson [32]). Westin [18] discusses whether or not any preferred spanwise scale exists that is most likely to be excited inside the boundary layer for any specific scale in the free stream. Fransson and Alfredsson [14] report a decrease of the spanwise scale inside the boundary layer with increasing *Tu* for a Blasius flow, and good agreement of the spanwise scale with spatially predicted OP-scales by Andersson et al. [34] and Luchini [27]. This study strengthens the hypothesis that for high enough *Tu* the boundary layer preferentially amplifies disturbances whose scales are close to that of the optimal disturbance. However, it should be remembered that the free stream scales are important and that the FST level does probably not set the spanwise scale inside the boundary layer by itself.

5. Conclusions

The transient behaviour of small disturbances in the asymptotic suction boundary layer (ASBL) has been investigated using a direct-adjoint approach in the temporal framework which is exact for this parallel flow. Initial disturbance configurations (optimal perturbations, OP) are found which maximize subsequent algebraic amplification of perturbation kinetic energy over a given period.

Significant algebraic growth is shown to occur, albeit less than that occurring in the Blasius boundary layer, which represents the no suction case. The difference can be attributed to the change in shape of the mean streamwise velocity profile. On the other hand, algebraically excited disturbances are shown to persist longer in the ASBL.

In accordance with other results for two-dimensional boundary layer flows, most growth occurs for disturbances which are infinitely elongated in the streamwise direction. These OP initially take the form of streamwise-oriented vortices which engender streaks, or large variations in the streamwise disturbance velocity. When scaled by momentum thickness, the spanwise wavenumber of the disturbance experiencing maximum amplification is identical to that for the Falkner–Skan family of boundary layers.

The numerical results from this work are in good agreement with experimental data obtained by Fransson [32]. That is, the velocity profile of the streak resulting from the OP undergoing the most growth is in good agreement with disturbances measured in the ASBL. The agreement is slightly better for the optimal perturbation whose spanwise wavenumber matches the streak spacing observed experimentally. Streak spacing in the experiment appears to be dependent on *Tu*. As the FST level increases, the streak spacing approaches the numerically determined wavenumber for the disturbance undergoing the most growth.

The asymptotic suction boundary layer is a suitable model for flows which may result from active flow control via steady suction (Walther et al. [11], Pralits et al. [10]), amongst other applications. This work shows that algebraic disturbance amplification is a viable linear path to transition in the ASBL, and that OP for this class of flow must be taken into consideration in applications.

Acknowledgements

The authors would like to thank Profs. P.H. Alfredsson, A. Bottaro, and P. Luchini for valuable comments which lead to an improved manuscript. J.H.M. Fransson's stay in Toulouse was supported by an EU Marie Curie Training Site Fellowship in addition to his basic foundation by The Swedish Research Council (VR).

References

[1] H. Schlichting, Boundary Layer Theory, McGraw-Hill, 1979.
[2] T.R. Bewley, Flow control: new challenges for a new renaissance, Progr. Aerospace Sci. 37 (2001) 21–58.
[3] P. Moin, T.R. Bewley, Feedback control of turbulence, part 2, Appl. Mech. Rev. 47 (6) (1994) S3–S13.
[4] R.D. Joslin, G. Erlebacher, M.Y. Hussaini, Active control of instabilities in laminar boundary layers – overview and concept validation, J. Fluids Engrg. 118 (3) (1996) 494–497.
[5] R.D. Joslin, Aircraft laminar flow control, Annu. Rev. Fluid Mech. 30 (1998) 1–29.
[6] J. Lumley, P. Blossey, Control of turbulence, Annu. Rev. Fluid Mech. 30 (1998) 311–327.
[7] P. Balakumar, P. Hall, Optimum suction distribution for transition cotnrol, Theor. Comput. Fluid Dynamics 13 (1999) 1–19.

[8] M. Högberg, Optimal control of boundary layer transition, Ph.D. Thesis, KTH, Stockholm, TRITA-MEK Tech. Rep. 2001:13, ISRN KTH/MEK/TR-01/13-SE.
[9] F. Lundell, Experimental studies of bypass transition and its control, Ph.D. Thesis, KTH, Stockholm, TRITA-MEK Tech. Rep. 2003:03, ISRN KTH/MEK/TR-03/03-SE.
[10] J. Pralits, A. Hanifi, D.S. Henningson, Adjoint-based optimization of steady suction for disturbance control in incompressible flows, J. Fluid Mech. 467 (2002) 129–161.
[11] S. Walther, C. Airiau, A. Bottaro, A methodology for optimal laminar flow control, submitted.
[12] F. Abergel, T. Témam, On some control problems in fluid mechanics, Theor. Comput. Fluid Dynamics 1 (1990) 303–325.
[13] T.R. Bewley, S. Liu, Optimal and robust control and estimation of linear paths to transition, J. Fluid Mech. 365 (1998) 305–349.
[14] J.H.M. Fransson, P.H. Alfredsson, On the disturbance growth in an asymptotic suction boundary layer, J. Fluid Mech. 482 (2003) 51–90.
[15] P.G. Drazin, W.H. Reid, Hydrodynamic Stability, Cambridge University Press, 1981.
[16] P.J. Schmid, D.S. Henningson, Stability and Transition in Shear Flows, Springer, 2001.
[17] L.M. Hocking, Non-linear instability of the asymptotic suction velocity profile, Quart. J. Mech. Appl. Math. 28 (1975) 341–353.
[18] J. Westin, Laminar-turbulent boundary layer transition influenced by free stream turbulence, Ph.D. Thesis, KTH, Stockholm, TRITA-MEK Tech. Rep. 1997:10, ISRN KTH/MEK/TR-97/10-SE.
[19] M. Matsubara, P.H. Alfredsson, Disturbance growth in boundary layers subjected to free-stream turbulence, J. Fluid Mech. 430 (2001) 149–168.
[20] K.M. Butler, B.F. Farrell, Three-dimensional optimal perturbations in viscous shear flow, Phys. Fluids A 4 (1992) 1637–1650.
[21] T. Ellingsen, E. Palm, Stability of linear flow, Phys. Fluids 18 (1975) 487–488.
[22] M.T. Landahl, A note on an algebraic instability of inviscid parallel shear flows, J. Fluid Mech. 98 (1980) 243–251, 1637–1650.
[23] L.S. Hultgren, L.H. Gustavsson, Algebraic growth of disturbances in a laminar boundary layer, Phys. Fluids 24 (1981) 1000–1004.
[24] L.H. Gustavsson, Energy growth of three-dimensional disturbances in plane Poiseuille flow, J. Fluid Mech. 224 (1991) 241–260.
[25] S.C. Reddy, D.S. Henningson, Energy growth in viscous channel flows, J. Fluid Mech. 252 (1993) 209–238, 1637–1650.
[26] L.N. Trefethen, A.E. Trefethen, S.C. Reddy, T.A. Driscoll, Hydrodynamic stability without eigenvalues, Science 261 (1993) 578–584.
[27] P. Luchini, Reynolds number independent instability of the boundary layer over a flat surface: optimal perturbations, J. Fluid Mech. 404 (2000) 289–309.
[28] E. Reshotko, Transient growth: A factor in bypass transition, Phys. Fluids 13 (2001) 1067–1075.
[29] P. Andersson, L. Brandt, A. Bottaro, D.S. Henningson, On the breakdown of boundary layer streaks, J. Fluid Mech. 428 (2001) 29–60.
[30] P. Corbett, A. Bottaro, Optimal perturbations for boundary layers subject to stream-wise pressure gradient, Phys. Fluids 12 (2000) 120–130.
[31] P. Corbett, A. Bottaro, Optimal linear growth in swept boundary layers, J. Fluid Mech. 435 (2001) 1–23.
[32] J.H.M. Fransson, Investigations of the asymptotic suction boundary layer, Lic. Thesis, KTH, Stockholm, TRITA-MEK Tech. Rep. 2001:11, ISRN KTH/MEK/TR-01/11-SE.
[33] F.M. White, Viscous Fluid Flow, McGraw-Hill, 1991.
[34] P. Andersson, M. Berggren, D.S. Henningson, Optimal disturbances and bypass transition in boundary layers, Phys. Fluids 11 (1999) 134–150.